Fatigue Fract. Engng Mater. Struct. Vol. 15, No. 1, pp. 43–56, 1992
Printed in Great Britain.

8756-758X/92 $5.00 + 0.00

ON THE RELATIONSHIP BETWEEN LOW CYCLE FATIGUE AND CRACK GROWTH RATE PROPERTIES IN WELDED STEEL COMPONENTS

BJØRN SKALLERUD
Division of Structural Engineering, SINTEF, N-7034 Trondheim, Norway

(Received in final form 21 February 1991)

Abstract—Previous investigations have shown that for plain materials, the crack growth rate constants applied in an elastic–plastic crack growth model may be obtained indirectly from the constants describing the low cycle fatigue capacity of the material. In the present study a simple EPFM crack growth model, based on bulk strain amplitude as the governing parameter, is assumed. The crack growth constants derived from the linear regression constants describing the LCF capacity of manually butwelded components are determined, and the validity of the resulting EPFM crack growth model is checked against measured LCF crack growth data.

NOMENCLATURE

a = crack depth
a_0, a_f = initial and final crack depth
da/dN = crack growth rate
B = logarithm of final to initial crack size ratio
C_{1-4} = coefficients in crack growth relationships
c = fatigue ductility exponent
E = Young's modulus of elasticity
$F_{n'}$ = cyclic material behaviour dependent factor in J solution
F_s = surface and geometry factor in J solution
J = Rice's J-integral
ΔJ = cyclic J-integral
k_v = plane stress, plane strain correction factor in elastic J solution
ΔK = stress intensity factor range
n' = cyclic hardening exponent
$n1 \ldots n4$ = exponents in crack growth relationships
N = cycles
N_f = number of cycles to failure
$\Delta W_{p,\infty}$ = range of plastic strain energy density; distant from the crack
ϵ_a, ϵ_{pa} = total and plastic strain amplitude
ϵ'_f = fatigue ductility coefficient for total strain amplitude
ϵ'_{fp} = fatigue ductility coefficient for plastic strain amplitude
$\Delta\epsilon_p$ = plastic strain range
ν = Poisson's ratio

Abbreviations

AWS = American Welding Society
CT = compact tension
EPFM = elastic–plastic fracture mechanics
FEM = finite element method
HAZ = heat affected zone
HCF = high cycle fatigue
LCF = low cycle fatigue
LEFM = linear elastic fracture mechanics

INTRODUCTION

Damage assessments of highly strained structural components, e.g. in critical joints in a damaged offshore platform, may be performed by employing plastic strain range as a damage parameter in combination with a damage accumulation model. Often, the linear damage accumulation model according to Miner and Palmgren [1, 2] is assumed. This assumption is reasonable in low cycle fatigue situations, where the crack initiation phase is small and the major part of the fatigue life consists of crack growth [3–7], i.e. the significant sequence effects associated with summation of damage due to different types of damage processes in the crack nucleation–micro crack growth phase and the macro crack growth phase are circumvented [8]. When the damage sum equals unity, a predefined failure state is reached. This state may correspond to the creation of a crack of a few millimeters.

An improved measure of the current damage situation in a component may be determined if one applies crack depth as the damage parameter, and integrates a crack growth relationship through the load history the component is subjected to. Several elastic–plastic crack growth models have emerged over the last decades. One approach is based on the cyclic version of the J-integral [6, 9–11]. Another approach is based on some strain parameter as the governing crack growth parameter [3, 12–14]. These crack growth models have shown to be applicable in predicting the crack growth in LCF situations. Kaisand and Mowbray showed that the fatigue crack growth parameters employed in the elastic–plastic crack growth model based on the cyclic J-integral could be derived from the parameters describing the LCF capacity of the material (and vice versa) [15]. This approach was motivated from the fact that the determination of the LCF capacity parameters is much simpler than obtaining the EPFM crack growth parameters directly from evaluation of measured crack development.

In the present investigation this indirect method of obtaining the crack growth parameter is further explored with respect to manually buttwelded steel plates axially loaded in the LCF regime. A strain based crack growth model is assumed [16].

ELASTIC–PLASTIC CRACK GROWTH MODELS

The range of the elastic stress intensity factor may be applied as the governing parameter in fatigue crack growth situations under nominally elastic conditions, and when the plastic zone around the crack tip is small compared to the crack length and the remaining ligament of the component. In this case, ΔK characterizes the crack tip stress and strain field, hence also the cyclic plasticity occurring in this region. If the requirements listed above are not met, the cyclic J-integral, ΔJ, may be employed in an analogous manner, i.e. ΔJ is assumed to characterize the crack tip stress and strain field and control the damage processes occurring in the crack tip region. Dowling and Begley introduced the EPFM crack growth model [10] of the form

$$\frac{da}{dN} = C_1 \Delta J^{n1} \tag{1}$$

and crack growth in CT specimens was described satisfactorily [10]. Later Dowling showed that equation (1) was a geometrically independent crack growth relationship for high strain loading in four different types of specimens [5]. The methodology for life predictions based on equation (1) is developing [6, 11, 17]. There are still some problems that remain to be resolved: analytic plastic J-solutions for practical crack shapes and structural geometries; anomalous crack growth

behaviour for small cracks (as occurs for the growth of small cracks if described by ΔK at lower stress levels); non-stationary crack closure behaviour [18].

The crack growth constants C_1 and $n1$ may be obtained indirectly in two ways. First, the connection between ΔJ and ΔK in the LEFM long crack regime may be used ($\Delta J = \Delta J_e + \Delta J_p \approx \Delta J_e$):

$$\Delta J = k_v \frac{\Delta K^2}{E} \tag{2}$$

$$\frac{da}{dN} = C_2 \Delta K^{n2} = C_1 (k_v \Delta K^2/E)^{n1} \tag{3}$$

where k_v is equal to 1 in plane stress, and equal to $1 - \nu^2$ in plane strain. Hence, the EPFM crack growth constants are derived from the LEFM constants. This approach may, however, introduce inaccuracies due to different crack closure in high strain fatigue growth of small cracks and in LEFM growth of long cracks [19]. An improvement of this situation may be obtained by using the effective values of the cyclic K and J, but still deviations may occur due to non-stationary closure in the growth of small fatigue cracks. Second, one may employ the relationship between the LCF capacity as described in Refs [20, 21], i.e.

$$\epsilon_{pa} = \epsilon'_{pf}(2N_f)^c \tag{4}$$

The integrated expression for equation (1) if ΔJ is described through the remote plastic strain energy density range $\Delta W_{p,\infty}$ [15, 22] ($\Delta J \approx \Delta J_p$):

$$\Delta J_p = F_s F_{n'} \Delta W_{p,\infty} a \tag{5}$$

where F_s is a factor accounting for crack shape and component geometry, and $F_{n'}$ depends on the cyclic strain hardening exponent. Combining equations (1) and (5) and separation of variables lead to the following expression:

$$\int_{a_0}^{a_f} \frac{da}{a^{n1}} = C_1 (F_s F_{n'} \Delta W_{p,\infty})^{n1} \int_0^{N_f} dN. \tag{6}$$

Here it is assumed that F_s does not depend on crack depth, which may be too simplistic (at least for LEFM conditions [23]). The connection between ϵ_{pa} and $\Delta W_{p,\infty}$ may be obtained when the cyclic stress–strain curve is known [15]. Integrating the left side of equation (6) from an initial crack size to a crack size representing failure is equivalent to integrating the number of cycles on the right side from zero to failure, assuming that all of the fatigue life is consumed in propagating the crack. The initial and failure crack size should correspond to those representative of the LCF components used in determination of equation (4).

For welded components, the ΔJ approach becomes difficult to apply, mainly for two reasons. First, the crack usually grows in a region of changing material properties, which may be interpreted as singularities within and on the contour surrounding the crack tip on which the J-integral is developed; hence, a fundamental requirement for the derivation of the J-integral is not met [24]. Second, the crack shape may be very complex, as will be illustrated subsequently.

The EPFM crack growth approach based on bulk plastic strain range leads to simple expressions for crack growth, e.g. [12, 3, 14, 25]:

$$\frac{da}{dN} = C_3 \Delta \epsilon_p^{n3} a. \tag{7}$$

In employing such a crack growth relationship, the geometry independence is lost, and the constants C_3 and $n3$ reflect the influence of the shape of the crack and other geometrical characteristics. Krawinkler and Zohrei determined successfully a relationship of the equation (7) type for the description of crack growth in welded I-beams [25]. LCF testing of welded components have shown that the scatter in the results is reduced when the number of cycles to failure is correlated to total strain amplitude instead of plastic strain amplitude [26]. Hence, the LCF capacity for a welded component may be described by [16]:

$$\epsilon_a = \epsilon_f'(N_f)^c \tag{8}$$

and the corresponding EFPM crack growth model may be described by [16]:

$$\frac{da}{dN} = C_4 \epsilon_a^{n4} a. \tag{9}$$

Separation of variables and integration of each side may then be performed:

$$\int_{a_0}^{a_f} \frac{da}{a} = C_4 \epsilon_a^{n4} \int_0^{N_f} dN \tag{10}$$

$$\ln \frac{a_f}{a_0} = B$$

$$\text{hence } \frac{B}{C_4} = \epsilon_a^{n4} N_f. \tag{11}$$

Comparing equations (11) and (8) leads to

$$n4 = \frac{-1}{c} \tag{12}$$

$$C_4 = B(\epsilon_f')^{1/c} \tag{13}$$

i.e. the crack growth constants are obtained from the LCF constants. The crack growth coefficient now depends on initial and final crack size; they should be representative of those in the components tested with respect to LCF. A possible dependency of crack depth on the crack growth coefficient is neglected. If total strain range is applied in equation (8), the strain range has to be applied in equation (9) also if the coefficient is calculated from equation (13) with an LCF regression coefficient based on strain range.

EXPERIMENTAL INVESTIGATION

Materials and test specimen

In the present investigation an St 52-3N normalized structural steel was used as base material. Measured chemical and mechanical properties are listed in Table 1. The welding electrodes chosen for the buttwelds were classified according to AWS A5.1:E 7028 (see Table 1). The test specimens originated from the same batch and were tested with the longitudinal axis parallel to the rolling direction. The 20 mm thick plates were cut into 225 mm wide specimens, welded manually at the midsection and machined to the shape shown in Fig. 1(a). Hence, start–stop points in the weldment were removed, and residual stresses were released due to the reduced constraint. A linear elastic FEM analysis of the specimen revealed no stress concentration at the midsection caused by the

Table 1. Chemical composition (% wt) and mechanical properties data for base and weld metal

	C	Si	Mn	P	S	Cu	Ni
Base metal	0.19	0.39	1.49	0.013	0.007	0.01	0.03
Weld metal	0.08	0.35	0.91	0.014	0.007	0.01	0.03
	Cr	Mo	V	Ti	Nb	Al	H
Base metal	0.02	0.01	0.01	0.001	0.002	0.035	0.00009
Weld metal	0.03	0.01	0.02	0.02	0.003	0.002	0.00005

	σ_y(MPa)	σ_{UTS}(MPa)	ϵ_f
Base metal	375	550	29%
Weld metal	408	513	26%

...al width variation. The weld geometry was of the X-type. No preheating of the specimens was performed, and the specimens were not annealed after welding. Figure 1(b) depicts a typical weld geometry shape, i.e. a relatively smooth weld toe region.

The plates were mounted in a special rig with heavy anti-buckling arrangements in order to preclude local buckling of the axially loaded specimens [16]. The specimens were subjected to strain controlled loading, with one extensometer attached on each side of the specimen (see Fig. 1). The strain R-ratio was held at -1 during the testing, and the loading frequency was in the range of 1.2–4.2 cycles/min. Hence, the base metal strain close to the weldment was employed as the

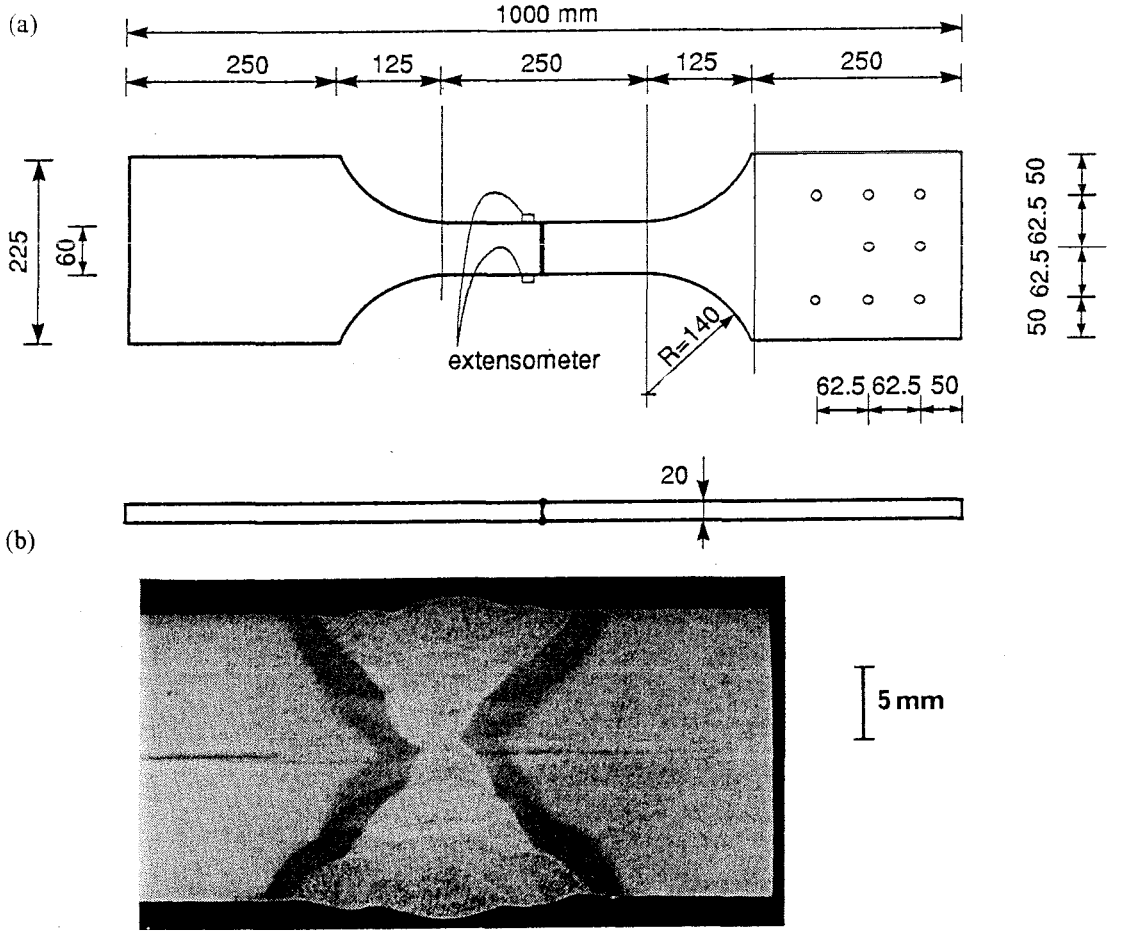

Fig. 1. Test specimen and buttweld geometry.

Table 2. LCF capacities of buttwelded steel plates

Specimen No.	ϵ_a(%)	N_f(cycles)	Frequency (1/s)
1	1	292	0.055
2	1.3	80	0.035
3	0.5	2617	0.07
4	0.8	410	0.035
5	0.8	542	0.05
6	0.7	504	0.07
7	1	211	—
8	0.5	1107	0.08
9	0.5	1131	0.09
11	0.7	450	0.05

governing parameter for description of crack growth and LCF capacity. The LCF capacity for this specimen type was obtained from testing ten specimens at room temperature. Significant crack development during the final stages of testing was detected in some of the specimens when the tensile load amplitude decreased. In such cases, a 20% reduction in tensile load determined the failure criterion, and the specimens were statically fractured at this stage. If no significant decrease in tension load was observed, total separation of the specimen due to cyclic loading determined the LCF life.

Test results

In Table 2 the LCF results for the axially loaded specimens are listed, and Fig. 2 shows the test results and the linear regression curve. The linear regression constants in equation (8) were calculated as $\epsilon_f' = 0.055$ and $c = -0.32$. In addition, the regression lines for the LCF capacity of the base material and weld metal are plotted in Fig. 2 for comparison [16]. The cyclic stress–strain curves of these materials were close, and consequently the strain in the weld in the plates was of the same magnitude as the base metal strain when subjected to the same stress level. Figure 2 shows

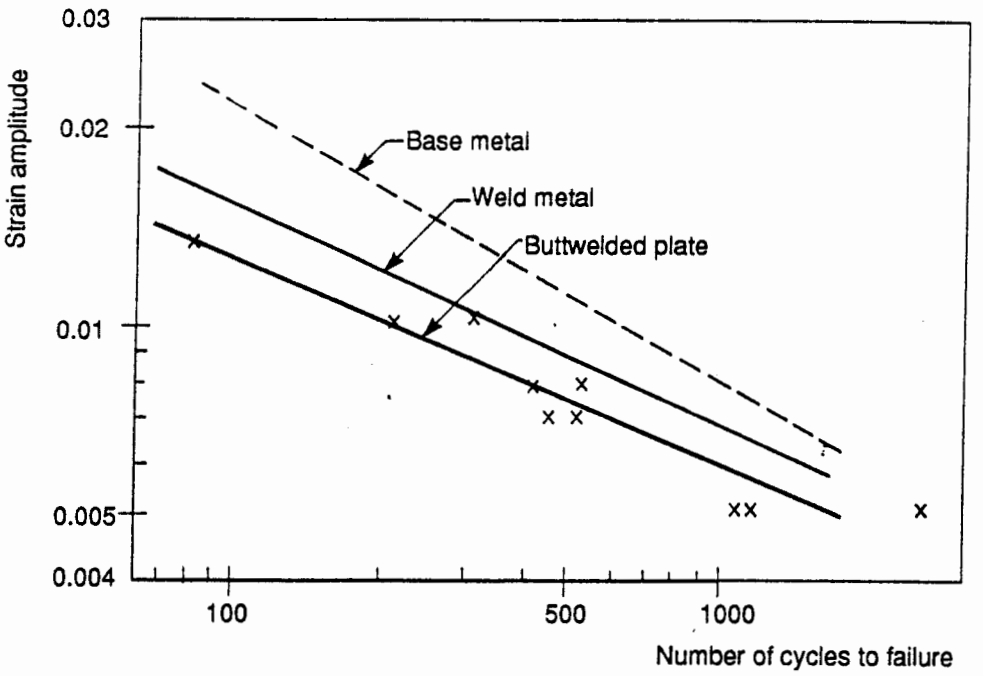

Fig. 2. LCF capacity of buttwelded plates, base and weld metal.

that the LCF capacity of the weld metal to a large extent determined the LCF capacity of the welded plates. The cyclic material behaviour has been reported elsewhere [27, 28].

Figures 3 and 4 illustrate how the cracks developed in some of the specimens. For specimen 1 (ϵ_a, $N_f = 292$), the dominant crack initiated from an inclusion located in the middle of the weld and grew outwards in an elliptical manner. This behaviour also occurred in specimen 2 ($\epsilon_a = 1.3\%$, $N_f = 80$). In specimen 3 ($\epsilon_a = 0.5\%$, $N_f = 2617$), two cracks grew from each side of the

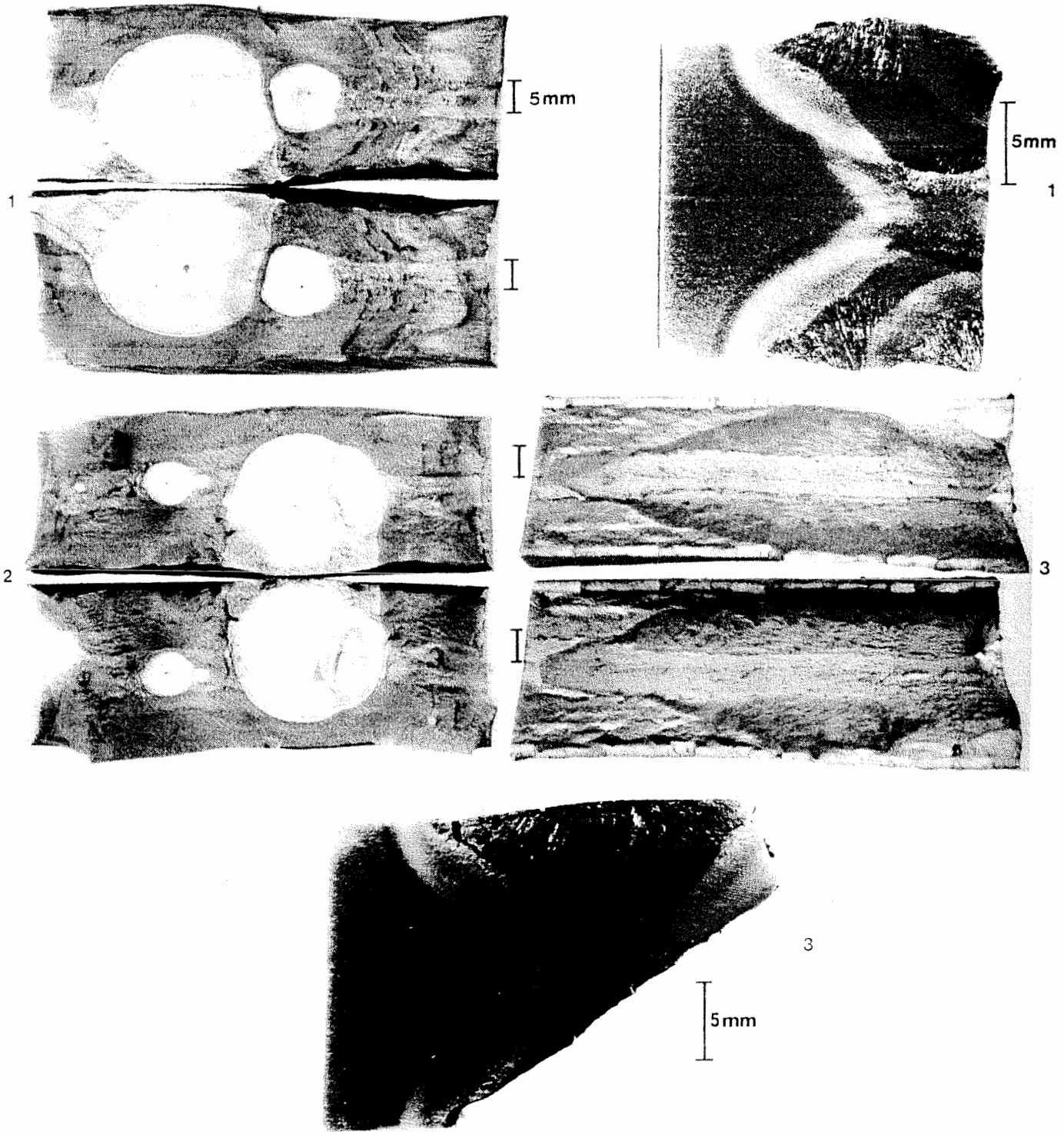

Fig. 3. Crack initiation and growth in the buttwelded plates.

weldment in the HAZ region, then some crack growth developed along the fusion line (Fig. 3). Figure 4 illustrates the complexity of the crack development located in the weld metal of specimen 6 ($\epsilon_a = 0.7\%$, $N_f = 504$), whereas for specimen 9 ($\epsilon_a = 0.5\%$, $N_f = 1131$), the dominant crack grew from the weld toe through HAZ and into the base metal. One observation from the results was that although the cracks grew with different shapes in different specimens loaded with the same strain amplitude, the LCF life was relatively little influenced.

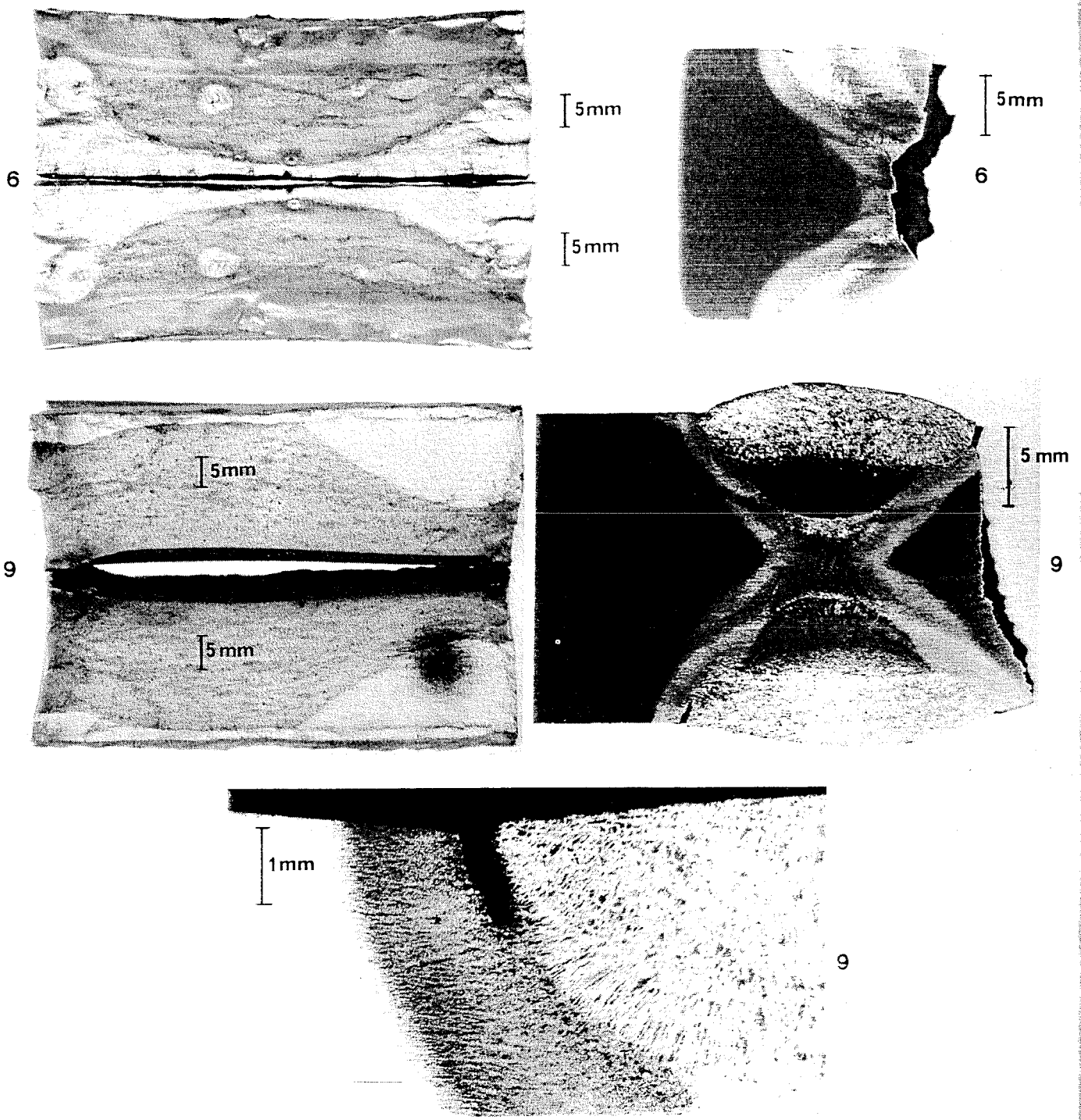

Fig. 4. Crack initiation and growth in the buttwelded plates, continued.

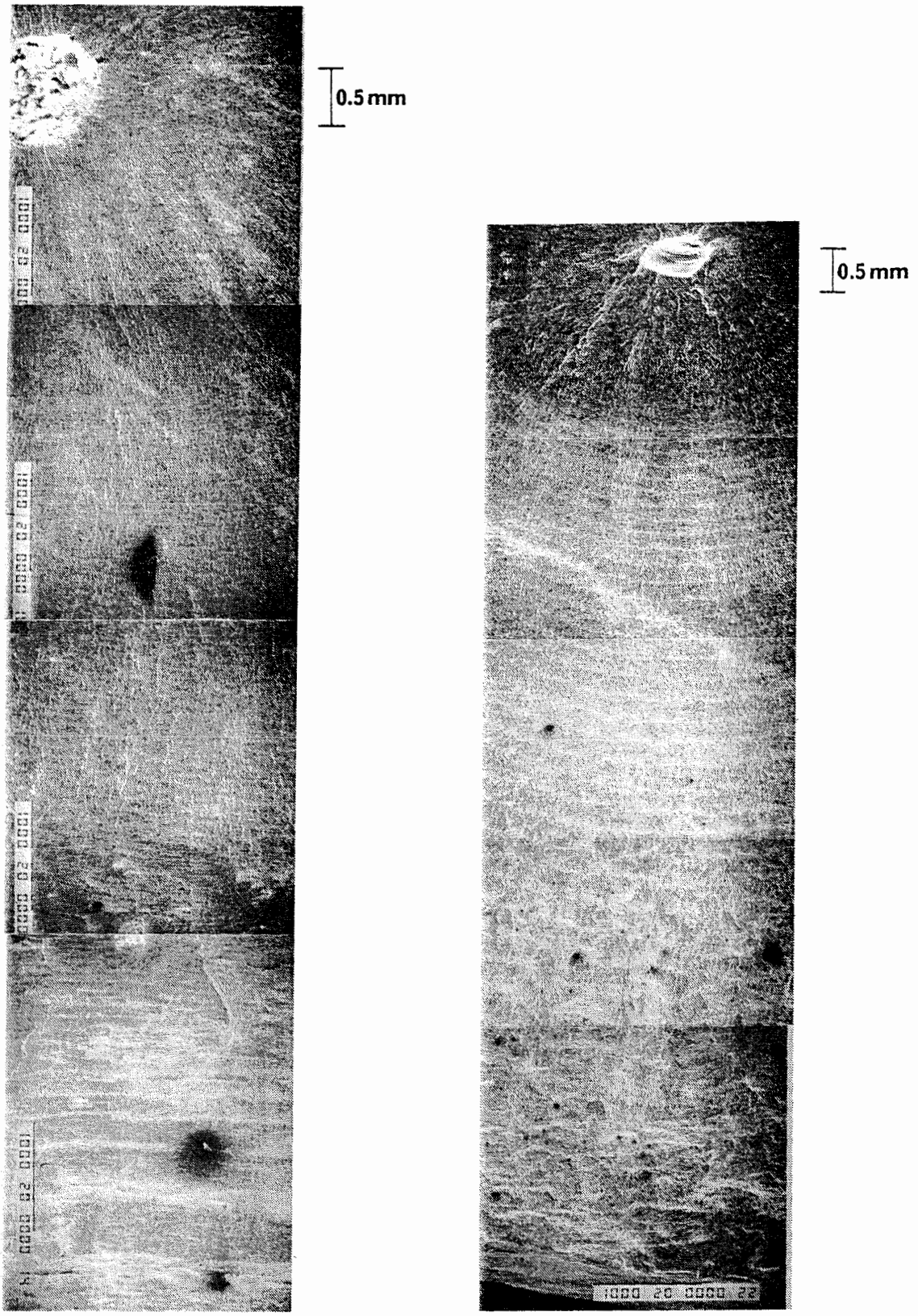

Fig. 5. Striation patterns in specimens 1 and 2.

The detailed crack growth was evaluated through examination of the fractured surfaces in a scanning electron microscope. Figure 5 depicts the crack growth from the inclusions of specimens 1 and 2 and out to the surface of the plates. From these photos the crack size could be measured, and the corresponding number of cycles was counted. The crack fronts are visible from a striation-like pattern, but striation is probably not the correct term to use as the crack grew by some ductile tearing mechanism at these high load levels. In Fig. 6 the ln a–N regression lines and test data for specimens 1 and 2 are plotted, showing a linear correlation between ln a and N. Here a is the crack size according to the minor axis of the elliptical cracks. Equation (9) describes this behaviour for a given strain amplitude. When the regression lines are extrapolated back to $N = 0$, a measure of initial crack size is obtained. These values, 0.04 and 0.15 mm, correspond reasonably well with the size of the inclusions shown in Fig. 5.

When the crack growth constants of equation (9) are determined from the LCF capacity constants according to equations (12) and (13), the following crack growth relationship is obtained for the butterwelded plates (mm/cycle, mm):

$$\frac{da}{dN} = 3.56 \times 10^4 \epsilon_a^{3.09} a. \tag{14}$$

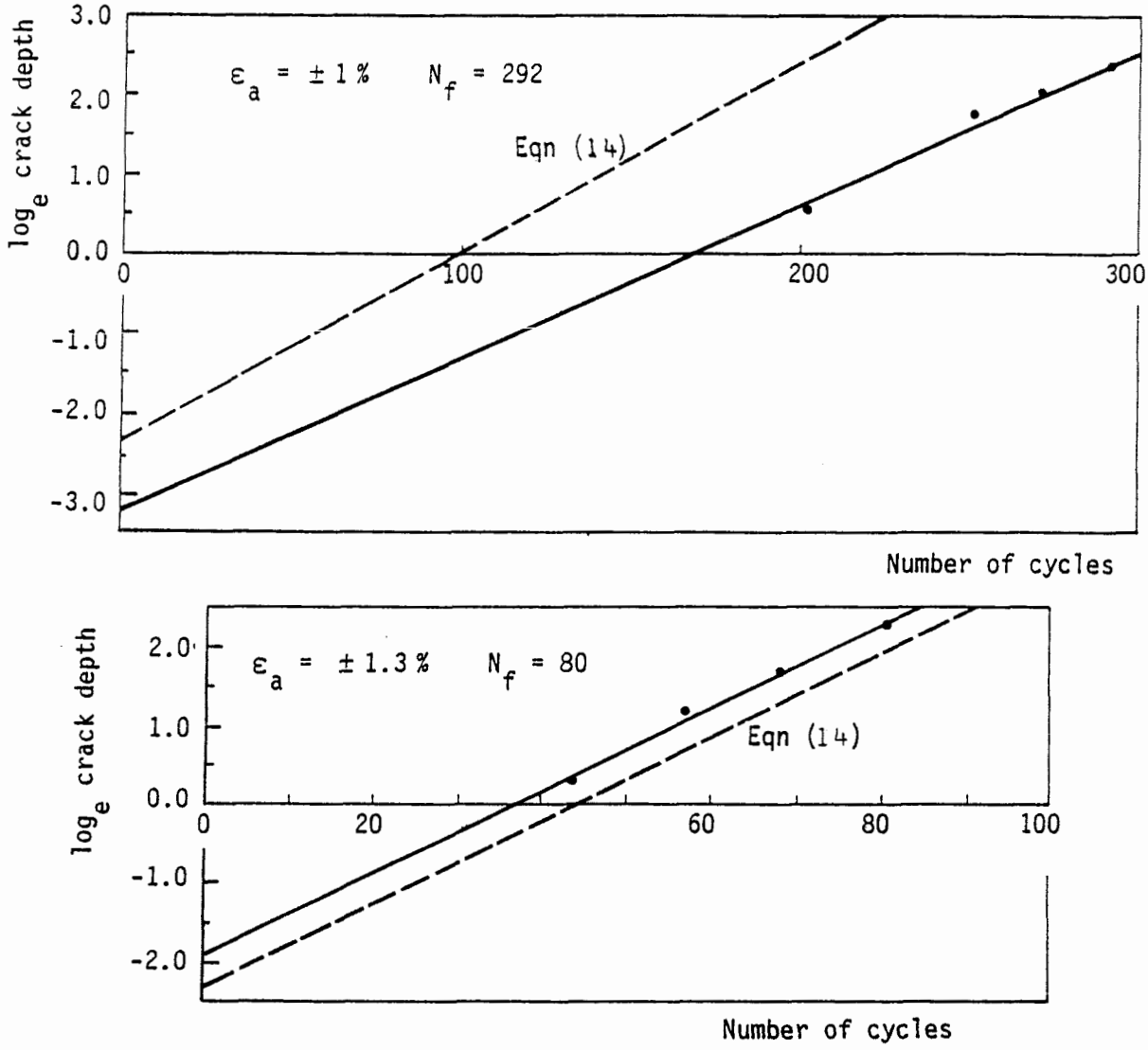

Fig. 6. Crack depth in thickness direction (ln a mm) vs cycles for specimens 1 and 2.

Here the initial crack size is taken as 0.1 mm, and the final crack size 10 mm, i.e. half of the specimen thickness. The broken lines in Fig. 6 are determined from equation (14) for the corresponding strain amplitudes, and equation (14) yields the solid line in Fig. 7. Since $d \ln a/dN$ is dimensionless with respect to length, the regression coefficient does not depend on this dimension, and the dimensions for crack length may be chosen for convenience. Unfortunately, the detailed crack growth development could only be evaluated for specimens 1 and 2, resulting in the two points in Fig. 7. If one assumes that the exponent 3.09 is representative, i.e. a negative inverse relationship exists between the slope of the LCF capacity curve and the slope of the EPFM crack growth curve, the two broken lines in Fig. 7 correspond to the initial and final crack sizes indicated, i.e. (0.01 and 20 mm) and (0.5 and 5 mm). These lines illustrate that the influence of uncertainties connected with the determination of the initial and final crack sizes are relatively low.

In order to obtain a comparison with more test results, other published data is evaluated subsequently.

Tests performed by Krawinkler and Zohrei

In [25] the LCF capacity of cantilever I-beams welded to a heavy girder and loaded in cyclic plastic bending was determined. The objective was to assess structural damage due to severe earthquakes according to LCF methodology. The crack growth was also measured in the six specimens used in the constant amplitude test program. The experimentally obtained LCF capacity and EPFM crack growth relationship were [25]:

$$\Delta\epsilon_p = 0.158 N_f^{-0.47} \tag{15}$$

$$\frac{da}{dN} = 130\,\Delta\epsilon_p^{1.91}\, a. \tag{16}$$

Here a is the crack depth measured from the outside of the flange and into the thickness, and $\Delta\epsilon_p$ is the plastic strain range in the base metal measured close to the weldment. The experimental crack growth rates and their regression given by equation (16) (dotted line) are plotted in Fig. 8. The mean value of the initial crack size was estimated to be 0.04 mm [25]. Half of the flange

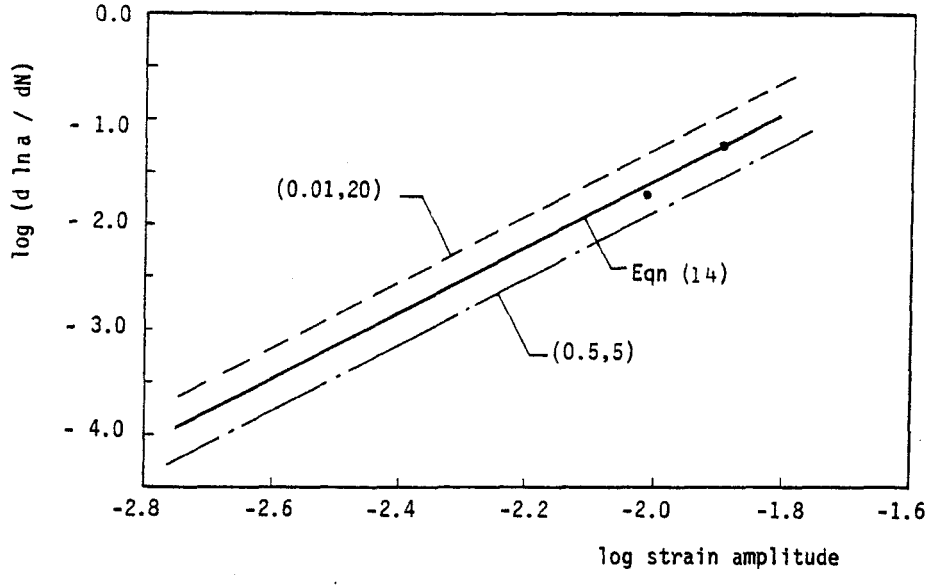

Fig. 7. Crack growth rate vs nominal strain amplitude for buttwelded steel plates for various initial and final crack sizes; the solid line is for $a_0 = 0.1$ mm and $a_f = 10$ mm.

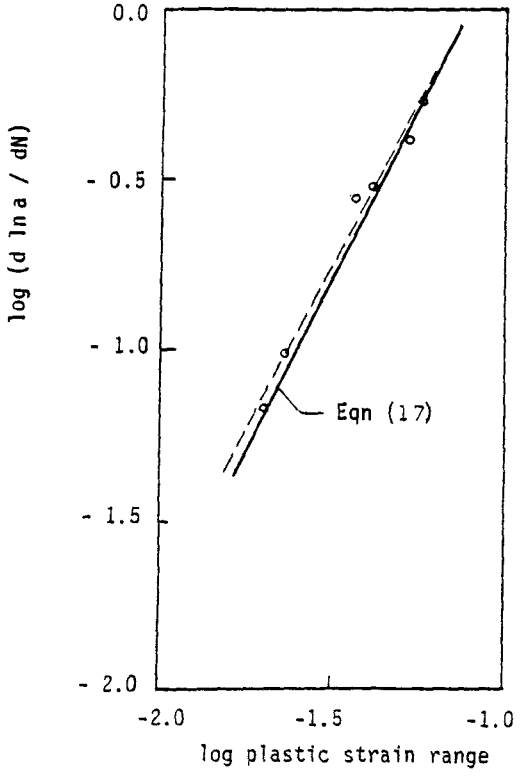

Fig. 8. Crack growth in welded cantilever I-beams [25].

thickness, 4.57 mm, was applied as fracture criterion, i.e. N_f corresponds to the the number of cycles to develop such a crack depth. Applying equations (12) and (13) led to the following EPFM crack growth relationship ($\Delta\epsilon \approx \Delta\epsilon_p$):

$$\frac{da}{dN} = 239\,\Delta\epsilon_p^{2.12}\,a. \tag{17}$$

The fully drawn line in Fig. 8 represents this relationship, and shows a very good correspondence with the measured crack growth data.

DISCUSSION

The previous section illustrated that the EPFM crack growth constants could be derived indirectly from the regression parameters describing the LCF capacity of the welded component, yielding good representation of the crack growth when compared with test data. From an engineering point of view, the simplicity of the approach is attractive.

When assessing LCF damage in welded components, one faces the problem of accounting for multiple crack initiation leading to complex crack shapes. Additionally, one has to analyse a crack growing in regions with changing material properties. These effects are implicitly accounted for in the LCF capacity constants, hence also in the derived crack growth constants.

The simple strain based approach leads to crack growth relationships that are geometry dependent. Therefore, LCF testing is required for different types of components in order to obtain EPFM crack growth models representative for the respective geometries and materials. The extent of this testing may seem to be a major disadvantage, but considering the experimental difficulty in measurement of elastic–plastic fatigue crack growth, the approach may still be applicable. If an

analytical method was established, leading to a geometry independent crack growth relationship, such testing could be minimized. An analytical model could also produce information on crack shape development. The simple method presented here does predict the crack shape, and the crack depth calculated from equation (9) should be regarded as an equivalent crack depth that may be compared with some critical crack size in order to assess the structural integrity. If a component initially is loaded in the HCF regime, one may assume that the continued crack shape development in the LCF regime follows the same pattern as initiated in the HCF loading period. The shape of HCF cracks in welded structures often has a semi-elliptical shape, this leads to a simple and well defined initial crack when the high strain loading commences.

One should note that the location of strain measurement and strain computation relative to the weldment should be the same if the component is subjected to a nominal strain gradient. Also, if total strain is employed as the governing parameter in the crack growth model, the crack growth constants reflect the range of fatigue lives obtained in the LCF tests. If equation (9) is applied in fatigue life predictions, the influence of the range of lives determined in the LCF test program on the crack growth parameters derived from the LCF parameters should be considered.

CONCLUSIONS

Some EPFM crack growth models were discussed, and the interrelations between the LCF capacity constants and the crack growth rate constants were described. A simple crack growth model based on bulk strain amplitude close to the weldment was employed in order to predict crack growth in buttwelded plates loaded in the LCF regime. The crack growth constants that were applied were determined from the LCF regression constants. A similar model based on the plastic strain range was also examined. Compared with the elastic–plastic crack growth experimental data, this simplified approach shows good correspondence, but the methodology has to be verified against more test data on other geometries, other combinations of weld/base metal, and variable load histories in order to determine if it is generally applicable or not.

REFERENCES

1. M. A. Miner (1945) Cumulative damage in fatigue. *J. appl. Mech.* **12,** A159.
2. A. Z. Palmgren (1924) Endurance of ball-bearings. *Z. Ver. dt. Ing.* **68,** 339.
3. H. D. Solomon (1972) Low cycle fatigue crack propagation in 1018 steel. *J. Mater.* **7,** 299–306.
4. D. F. Mowbray (1976) Derivation of a low cycle fatigue relationship employing the *J*-integral approach to crack growth, ASTM STP 601, pp. 33–46.
5. N. E. Dowling (1977) Crack growth during low cycle fatigue of smooth axial specimens, ASTM STP 637, pp. 97–121.
6. T. Hoshide, T. Yamada and S. Fujimura (1985) Short crack growth and life predictions in low cycle fatigue of smooth specimens. *Engng Fract. Mech.* **21,** 85–101.
7. Y. Murakami, S. Harada, T. Endo, H. Taniishi and Y. Fukushima (1983) Correlations among growth law of small cracks, low cycle fatigue law, and applications of Miner's rule. *Engng Fract. Mech.* **18,** 909–924.
8. K. J. Miller and M. F. E. Ibrahim (1981) Damage accumulation during initiation and short crack growth regimes. *Fatigue Engng Mater. Struct.* **4,** 263–277.
9. J. R. Rice (1968) A path independent integral and the approximate analysis of strain concentration by notches and cracks. *J. appl. Mech.* **35,** 379–386.
10. N. E. Dowling and J. A. Begley (1976) Fatigue crack growth during gross plasticity and *J*-integral, ASTM STP 590, pp. 82–103.
11. V. Bicego (1989) Low cycle fatigue life predictions in terms of an EPFM small crack model. *Engng Fract. Mech.* **32,** 339–349.

12. B. Tomkins (1986) Fatigue crack propagation—an analysis. *Phil. Mag.* **18,** 1041–1066.
13. R. C. Boettner, C. Laird and A. J. McEvily (1965) Crack nucleation and growth in high strain fatigue. *Trans. AIME* **233,** 379–387.
14. M. W. Brown (1986) Interfaces between short, long, and non-propagating cracks. In *The Behaviour of Short Fatigue Cracks* (Edited by K. J. Miller and E. R. de los Rios), pp. 423–439. Mechanical Engng Publications, London.
15. L. R. Kaisand and D. F. Mowbray (1979) Relationships between low cycle fatigue and fatigue crack growth rate properties. *J. Test. Eval.* **7,** 270–280.
16. B. Skallerud (1988) Cyclic plasticity and low cycle fatigue of structural steel and buttwelded components. Dr.ing. thesis, The Norwegian Institute of Technology, Trondheim.
17. H. Sehitoglu (1983) Fatigue life prediction of notched members based on local strain and elastic–plastic fracture mechanics concepts. *Engng Fract. Mech.* **18,** 609–621.
18. H. Obrtlik and J. Polak (1985) Fatigue growth of surface cracks in the elastic-plastic region. *Fatigue Fract. Engng Mater. Struct.* **8,** 22–31.
19. N. E. Dowling and N. S. Iyyer (1987) Fatigue crack growth and closure at high cyclic strains. *Mater. Sci. Engng* **96,** 99–107.
20. S. S. Manson (1954) Behaviour of materials under conditions of thermal stress. NACA TN 2933.
21. L. F. Coffin (1954) A study of the effects of cyclic thermal stress on a ductile metal. *Trans. ASME* **76,** 923.
22. C. F. Shih and J. W. Hutchinson (1976) Fully plastic solutions and large scale yielding estimates for plane stress crack problems. *J. Engng Mater. Technol.* **98,** 289–295.
23. B. Skallerud, O. I. Eide and S. Berge (1990) Fatigue crack growth in complex tubular joints. *IABSE Conf. Remaining Fatigue Life of Steel Structures*, Lausanne, pp. 209–218.
24. M. H. Bleakley, R. D. Jones and A. R. Luxmoore (1986) Path dependency of the Rice J-integral in weld geometries. ECF 6 (Edited by H. C. van Elst and A. Bakker), Vol. 1, pp. 643–654. Engineering Materials Advisory Services, Warley.
25. H. Krawinkler and M. Zohrei (1983) Cumulative damage in steel structures subjected to earthquake ground motions. *Computers Struct.* **16,** 531–541.
26. J. D. Harrison (1972) Low cycle fatigue tests on welded joints in high strength steels. Report C215/17/70, The Welding Institute.
27. B. Skallerud and P. K. Larsen (1989) A uniaxial cyclic plasticity model including transient material behaviour. *Fatigue Fract. Engng Mater. Struct.* **12,** 611–625.
28. B. Skallerud (1992) Constitutive modelling of cyclic plasticity and some implications for the computation of biaxial low cycle fatigue damage. SINTEF Report STF71 A89049. To appear in *Engng Fract. Mech.*